Chemical Sciences Journal
ISSN: 2150-3494

Gebreyesus Chem Sci J 2015, 6:2
DOI: 10.4172/2150-3494.100090

Research Article Open Access

Theoretical Comparison of O, S, Se and Te Terminal Active Site of Molybdo-Enzymes, In Terms of Their Property upon Reaction with Acetaldehyde

Sofani Tafesse Gebreyesus*

[1]*Department of Chemistry,College of Natural Sciences, Arbaminch University, Ethiopia.*

Abstract

Previous researches show that all members of chalcogene family could be a terminal in the molybdo-enzymes. But their structure as well as catalytic mechanism has not been studied much. In this paper, Density functional calculations have been performed on a model for the reductive half-reaction of the molybdo- enzymes containing Oxo, sulfido, sellenido and tellurido terminals, enabling a discussion of structural details of the Mo coordination sphere involved in the reaction with acetaldehyde.The reductive half reaction active sites, with oxo, sufido, sellenido and tellerido terminal truncated structures, were modeled using GaussView software. Energy, Mullikens charge, single negative frequency and bond descriptions of the complexes were among the very important tools obtained from the transition state structures, to study the properties of the active sites. In this work it has been found that the normalized energies for complexes with oxo, sulfido, sellenido and tellerido terminals were 433.923, 421.742, 419.284 and 403.0578 kcal/mol respectively. The decreasing trend found was the same, though the magnitudes of the energies differ significantly. The complex with oxo terminal shows considerably maximum energy barrier of 433.923 kcal in addition to its highest frequency. These are the evidence for its poor catalytic activity towards hydroxylation reaction. As a result of this and additional evidences from mulliken charge and bond length values, the reactivity of the active site towards acetaldehyde for its oxidation increases from active site with oxo to tellurido terminal. Besides, these findings give a clue for the possible natural existence of a molybdo-enzyme with Te-terminal.

Keywords: Density functional calculations; Molybdo- enzymes; Acetaldehyde; Mulliken charge; Single negative frequency.

Introduction

Studies show that in coordination with cofactors, molybdnium is the only second row transition metal that shows biological activity [1]. The study of reaction mechanisms of molybdo-enzymes as well as their structures started 50 years ago [2-8]. All enzymes in the xanthine oxidase family, which are found in many bacteria and animals, contain a structurally similar molybdopterin cofactor in the active site including Mo (VI to VI) center, an oxo group, a sulfido group, a dithiolene side chain to a pterin, and a water or hydroxide ligand (Figure 1.1). Theoretical modeling remains a problem because of the presence of all these molecules bonded to the metal center, but the reductive half structure has been shown crystallographically in the molybdo-enzyme [9-14]. These molybdo-enzymes catalyze hydroxylation reactions, the transfer of an oxygen atom between water and a substrate, which are ways to formulate the two-electron substrate and active-site regeneration reactions and may have mechanistic relevance [15]. Nicotinate catabolism in all organisms starts by enzyme Nicotinate De-Hydrogenase (NDH), which is found in anaerobic soil bacterium called E.barkeri [16,17]. Researches on the crystal structure of the active for NDH shows that selenium is bound as a terminal Mo-Se ligand to molybdenum instead of the terminal sulfido ligand in other molybdo-enzymes like xanthine oxidoreductase (XOR) [18]. Hence, in nature XOR and NDH are known to catalyze hydroxylation reaction on their physiological substrates. It is known that upon cyanide treatment of xanthine oxidase, its sulfur terminal could be removed as SCN^- and to be replaced by terminal oxygen, which is with no catalytic activity towards hydroxylation reaction [19]. All members of chalcogene family could be a terminal in these molybdo-enzymes, for example the substitution of tellurium has been achieved in other proteins, as shown in (Figure 1.2) [20]. Because of their biggest atomic size in the group, selenium and tellurium are expected to have better polarizability, good

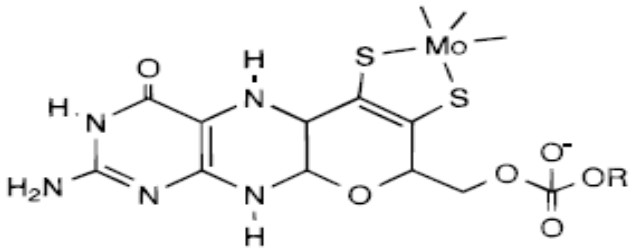

Figure 1.1: The structure of the molybdo-enzyme, in which Mo covalently bound to the dithionate moiety of a tricyclic pterin.

nucleophile and forms weak bond with molybdenum. Thus the catalytic activity of complex of active site with tellurium terminal of xanthine oxidase should be thoroughly studied so that it may give us information regarding its existence in nature. Especially in the cases of less reactive carbon centers, the increased reactivity may be important in catalyzing the oxidation or hydroxylation [21]. Since there is close similarity among these active sites, their catalytic activity would be compared and

***Corresponding author:** Sofani Tafesse Gebreyesus, Lecturer and researcher in Chemistry department, College of Natural Sciences, Arbaminch University, Ethiopia, Tel: + 251-46881-4986, Fax: +251-46881-0820/0279; E-mail: m sofani.tafesse@amu.edu.et/sofi.tafesse@yahoo.com

Received April 01, 2015; **Accepted** April 29, 2015; **Published** May 05, 2015

Citation: Gebreyesus ST (2015) Theoretical Comparison of O, S, Se and Te Terminal Active Site of Molybdo-Enzymes, In Terms of Their Property upon Reaction with Acetaldehyde. Chem Sci J 6: 90. doi:10.4172/2150-3494.100090

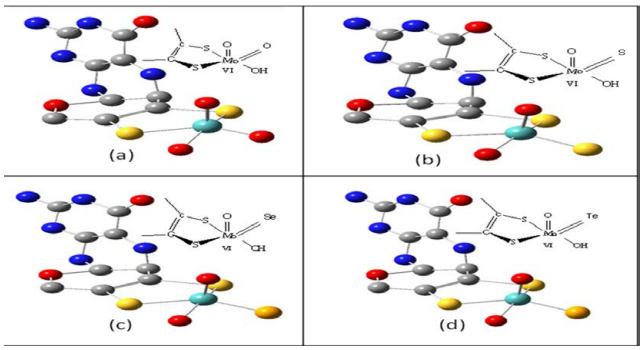

Figure 1.2: The primary coordination sphere for active sites with Oxo (a) Sulfido (b) Sellenido (c) and Tellerido (d) terminals of the reductive half-reaction.

the catalytic mechanism for active site with Sellenido terminal could be developed relating with mechanisms of XOR. In order to understand the events taking place during the mechanistic transformation, computational models are developed to evaluate the bonding and wave function descriptions. Using acetaldehyde as simple model substrate bound to the reductive half reaction active sites with oxo, sulfido, sellenido and tellerido terminals, the possible mechanism routes are developed. Thus selenium, oxygen or tellurium atom is incorporated in place of sulfido terminal of XOR enzyme and modeled a transition state structure for the transformation of tetrahedral reactant complex of the catalyst to the product bound intermediate, transfer of H from acetaldehyde to the terminals, as shown in Scheme 1.1 below, where X= O, S, Se or Te. The properties of these active sites with oxo, sulfido, sellenido and tellerido terminals are studied and compared.

Materials and Methods

Materials

All computational calculations were performed using Gaussian 03W (version 6.0) program software package (Gaussian, Inc., Wallingford, CT, USA). Molecular orbital and electronic structure visualization were performed using Gauss View 3.0 (Gaussian, Inc., Pittsburgh, PA, USA). The software was also used to compute the bond distances from the output files of the optimized structures. The pictorial views, for the frontier (HOMO and LUMO) orbitals, were generated from the checkpoint files using this software. The structures were initially developed using ChemDraw ultra 6.0 (Cambridge soft wares, Cambridge, MA, USA). All data were analyzed using Microsoft office excel 2003(Microsoft, Inc., Redmond, Washington, USA).

Methods

General computation procedure: Electronic structure calculations have been performed to generate Mulliken atomic charges (ΔqMo, ΔqS, etc.), total electronic energies, wave-function descriptions, bonding

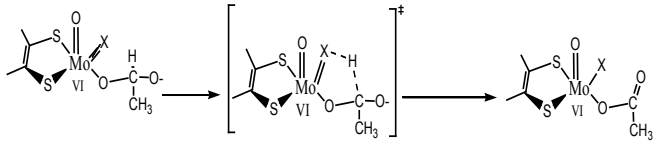

Scheme 1.1: A general structural model for the transition state.

descriptions, and bond orders. The parameters were generated from the geometry optimization, single point energy, frequency, and linear transit calculations. All computation calculations were performed using Gaussian 03W using density functional theory (DFT) method of the B3LYP, which is a hybrid exchange-correlation function with pure DFT and HF exchange function (DFT-B3LYP). The DFT method employing the B3LYP level of theory has been applied on the truncated analogue of the reductive half-reaction active site-bound to acetaldehyde. The 6-31G (d', p') basis set with a polarization function have been applied for non-metal atoms (C, H, O, S, and Se). Similarly, the LANL2DZ basis set and LANL2 effective core potentials have been applied for Mo and Te atoms, while running all sorts of calculations. Active site structures with a formula MoO (OH) X, where X is O, S, Se and Te have been modeled bonding with acetaldehyde using Gauss View. Initial structures of substrate-active site of all kinds have been optimized using "# b3lyp gen pseudo=read #p gfinputiop (6/7=3) opt pop=fullgfprint"key word, using Gaussian 03 software. Since the data for the model structures have been brought from Gauss view, the term "geom=connectivity" was used along with the key word, in order to specify the source of the molecule specification. In all complexes, the oxidation state of molybdenum was six, Mo (VI). Multiplicity for acetaldehyde bound complexes assigned 1. Both the charges and multiplicities were used to prepare the input files for electronic structure calculations. The initial optimized structures were used to set up input files for linear transit calculations by dividing the bond distance between hydrogen bound to the interaction site of acetaldehyde and the terminals X_{Mo} in to six to eight parts. Hydrogen from acetaldehyde was made to move towards the terminals (X_{Mo}). At each interval the X_{Mo}-H distance fixed and the structure was optimized. The job type "# opt=modredundant b3lypgen pseudo=read #p gfinputiop (6/7=3) pop=full gfprint" was used to optimize the structures. Only the word "modredundant" in the job type of linear transit calculation. The exact position of TS have been searched using # B3LYP gen pseudo=read #P GFINPUT IOP(6/7=3) opt=QST3" key word by combining the initial, final and initial guess structures for the presumed transition state structure.

The presence of transition state structure was verified by frequency calculation using "# b3lyp gen freq pseudo=read #p gfinputiop (6/7=3) pop=full gfprint" key word. With the presence of single negative frequency, the exact position of the transition state structure can be proved. In addition, the position of the transition state further was confirmed by an inflection point position of Mulliken charge profile of actively involving atoms of substrate-active site complex verses X_{Mo}-H bond distance. The Mulliken charges of the atoms were obtained from the output file of optimized structures of each complex. The transition state structure have been used as one input for the derivation of the overall mechanism and comparison with active sites having different terminals. Single point calculations have been carried out, for each proposed intermediate and transition state structures. After the optimization of the structures for both stepwise and concerted mechanisms, using the keyword "# b3lyp #p gen pseudo=readgfinput pop=full iop (3/33=1) gfprint". Molecular orbital and electronic structure visualization was performed using GaussView 3.0. The bond distances and angles have been computed from the output files of the optimized structures. The pictorial views, for the frontier (HOMO and LUMO) orbitals, have been generated from the checkpoint files using GaussView software.

Predicting the transition state structure: The prediction of transition state structures was carried out for the active sites with oxo, sulfido, sellenido and tellerido terminal bound to acetaldehyde, as

shown in Figure (2.2).

The input files for the linear transit optimization scans were developed using the X_{Mo}-$H_{acetaldehyde}$ distance, as a constraint. The difference in X_{Mo}-$H_{acetaldehyd}$ distance, between the initial ($C_{acetaldehyde}$-$H_{acetaldehyd}$ distance, when $H_{acetaldehyd}$ is bound to $C_{acetaldehyde}$) and the final distance (X_{Mo}-$H_{acetaldehyd}$ distance, when $H_{acetaldehyd}$ is bound to X_{Mo}), have been used to develop the intervals for the linear transit scans. A series of geometry optimizations have been carried out by stepping up the X_{Mo}-$H_{acetaldehyd}$ bond distance, at constant intervals.Once a series of structures are optimized, the total energies from each optimization steps were plotted against respective X_{Mo}-$H_{acetaldehyd}$ distances. From the plot, the structure with the highest energy was considered as an initial guess for locating the transition state structure. The input files containing the three geometries (the initial, final, and initial guesses) have been optimized. Optimization of the combined structures was used to generate a guess for the transition state structure, in terms of redundant internal coordinates, that are midway between Mo^{VI} and Mo^{IV} meta-stable states. The transition state structures have been located using the quadratic synchronous transit method (QST3). The final optimized geometries have been used as input files for the frequency and single point energy calculations. In addition, Mulliken atomic charges of major participating atoms of the active sites; Mo (molybdenum), O_{eq} (equatorial oxygen), O_{app} (apical oxygen), X_{Mo}, $H_{acetaldehyde}$ and C were computed. In addition the bond lengths were also calculated to justify the exact position of transition state structures. The structures of the four active sites with oxo, sulfido, sellenido and tellurido terminals and acetaldehyde were modeled separately and optimized as described above. Similarly, the structure of acetic acid was optimized. The approximate energy profile for the reactants, i.e.; four active sites with oxo, sulfido, sellenido and tellurido terminal and acetaldehyde, was computed from single point energy calculation which was carried out on the optimized structures. Similar calculation was performed for the product, using Mo-enedithiolate anion and the energies of the primary product, acetic acid. Transition state energies, which are obtained from the linear transit calculations, have been drawn relative to the reactants and products as shown in (Figure 2.1). Analyses of the electron density of the complexes were used, to show the degree of the orbital overlap and polarization of different bonds.

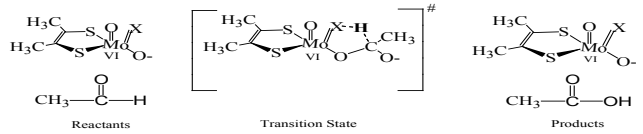

Figure 2.1: The reactants (acetaldehyde and active sites separately), TS and product (acetic acid and regenerated active sites separately) structures

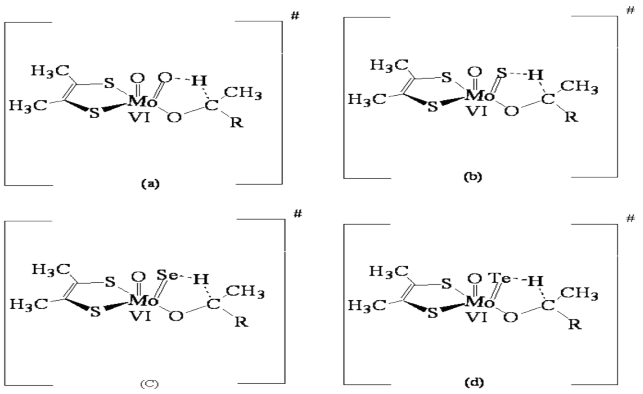

Figure 2.2: The geometries, representing the tetrahedral transition state structures.

Results and Discussion

The reductive half reaction active sites, with oxo, sufido, sellenido and tellerido terminal truncated structures, shown in Figure (2.2) were modeled using GaussView software. Energy, Mullikens charge and bond descriptions of the complexes were among the very important tools obtained from the transition state structures, to study the properties of the active sites. These were obtained by linear transit calculations were made to show the transfer of substrate bound to the active sites with terminals X (where X: O, S, Se or Te). Electron density and frequency were additional information that were obtained.

Total energy profile from linear transit scan

Though transition state has a fleeting existence, studies upon its formation and decay reveals crucial events taking place during catalytic activity of the catalyst on the substrate. Thus we modeled transition state complexes of the active sites with oxo, sulfido, sellenido and tellurido terminals. The transition state energy for the Transition State of active site with sulfido terminal was -1080909.936 kcal at S-H bond distance of 1.98539 angstrom (Figure 3.1). Whereas for active site with sellenido terminal was -2336399.53 kcal at Se-H bond distance

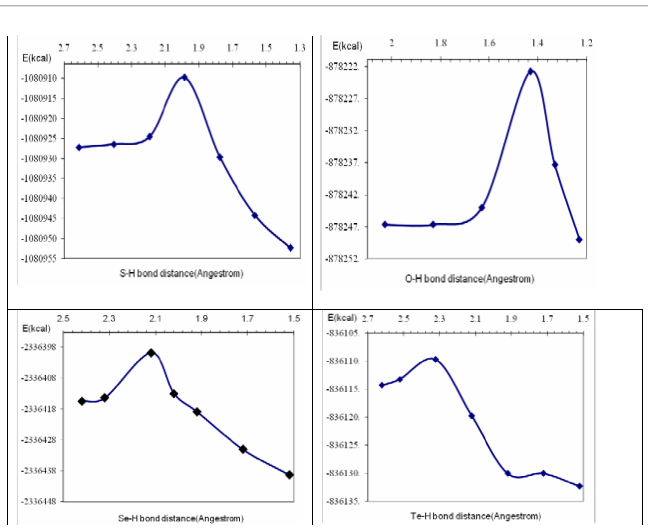

Figure 3.1: Total energy profile from linear transit scan.

of 2.11861 angstrom, for active site with oxo terminal was -878222.957 kcal at O_{Mo}-H bond distance of 1.43017 angstrom, while for with tellerido terminal the transition state energy was -836110.255 kcal at Te-H bond distance of 2.32158 angstrom.

Mulliken charge profile from linear transit calculation

The positions of the transition state structures were also located from inflections point shown in the Mulliken's charge profile on selected groups in the complex. The Mulliken charges were obtained from the output files of the optimized structures of each atom of the complexes. The change in Mulliken atomic charges of groups around the active site (S B, Mo, Oxo, O_{eq}, $C_{acetaldehyde,}$ S F, $H_{acetaldehyde}$ and X_{Mo})

as $H_{acetaldehyde}$ migrated from the $C_{acetaldehyde}$ of acetaldehyde (interaction site of acetaldehyde) to the X_{Mo} (X-H) terminals. For active sites with sellenido terminal, the Mulliken charge profile on S B, Mo, Oxo, O_{eq}, $C_{acetaldehyde,}$ S F, $H_{acetaldehyde}$ and Se_{Mo} of the active site has shown inflection at Se-H bond distance of 2.11861, which are the approximate position for the respective transition state structure (Figure 3.2). From coulombs law of force between charged objects, the bond energy directly proportional with the developing charge upon the two and is inversely related to the distance between them. The transfer of $H_{acetaldehyde}$ to selenium was proven from the decrease in positive Mulliken charge on molybdenum, while there is increase in positive Mulliken charge on $C_{acetaldehyde}$ of the substrate. Similarly the increase in Mulliken charge on $H_{acetaldehyde}$ is much larger for complexes of (0.142175 to -0.013786), (0.155155 to 0.155106), (0.111200 to -0.190735) for sulfido, Oxo and Tellerido terminated complex respectively.

Bond length Profile from linear transit calculation

The extent of Mo-Oeq bond elongation, in sulfido, oxo, and tellerido terminated transition state, extend by 7.093, 7.26, and 4.82 % respectively (Figure 3.3). The extent of shortening for O_{eq}- $C_{acetaldehyde}$ bond in complexes with Oxo, Sulfido and Tellerido terminals were by 15.09, 17.13 and 22.07% respectively. Likewise; the extent of Mo-S_{Mo}, Mo-O_{Mo} and Mo-Te_{Mo} bond elongation in substrate–active site at transition state extends by 0.693, 2.575 and 0.318 respectively. During the initial movement of $H_{acetaldehyde}$ transfer towards the terminals (X), Mo-O_{eq} bond becomes smaller but after the formation of the transition state, it became longer and longer and then broke eventually. The extent of Mo-Oeq bond elongation, in sellenido terminated transition state, extends by 7.605% to 1.76197 A°. According to Hammond Postulate, the transition state for an exothermic reaction occurs early along the reaction pathway so that it resembles the reactants[22] .The bond distances for the transition state of all active sites with oxo, sulfido, sellenido and tellerido terminals, could reveal shorter $C_{acetaldehyde}$ - $H_{acetaldehyde}$ bond and longer X_{Mo}-$H_{acetaldehyde}$ bonds, which are according to Hammond Postulate. This is proposed to indicate a substrate type transition state structure rather than a product type for all active sites with chalcogen terminal.

Intensity of the frequency is for the transition state structures of the active sites bound to acetaldehyde

The exact position of the transition state structures with highest energy were further proven by single imaginary negative frequency. This is to distinguish the minimum characterized by all other positive frequencies. Although the transition state structure characterized by one imaginary negative frequency, the imaginary negative frequencies and linear motions of the H_{RH}, at the transition state, also proposed to vary depending on the affinity of the terminals of the active site. According to Arrhenius equation activation energy and frequency factor are directly proportional. The frequencies for the acetaldehyde bound active site, with oxo, sulfido, sellenido and tellerido terminal, complexes in decreasing order are -875.042, -339.833, -721.35 and -318.56 respectively. It has been planned to compare the active sites with different terminals in terms of Mulliken charge and electron density profile on $H_{acetaldehyde}$, Mo-X bond lengths, energy profiles and frequency. The terminal that would be catalytically active and better reactive have to show increased charge on itself and hydrogen ion as the distance between them gets shorten. The negative mulliken charge on $H_{acetaldehyde}$ increases in acetaldehyde bound active site complex with sellenido terminal from 0.149153 to 0.0043 (Figure 3.2). Similarly, for complexes

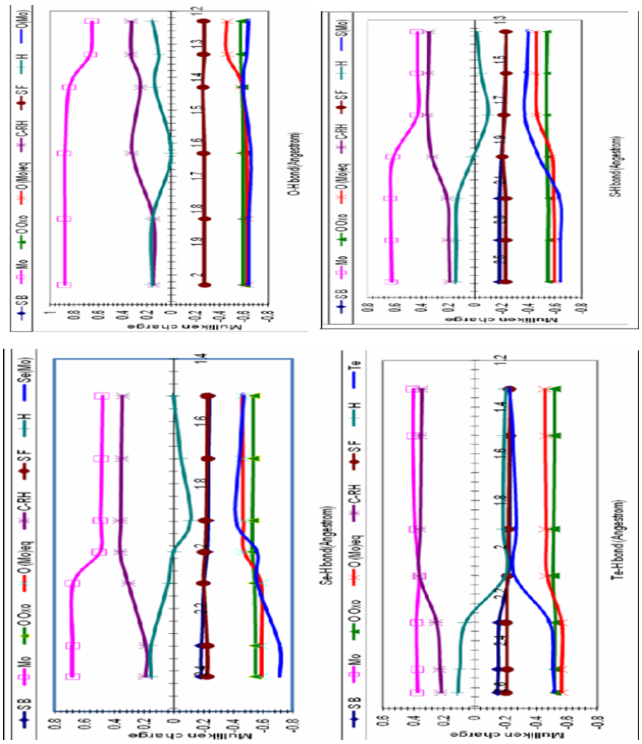

Figure 3.2: Mulliken charge profile from linear transit calculation.

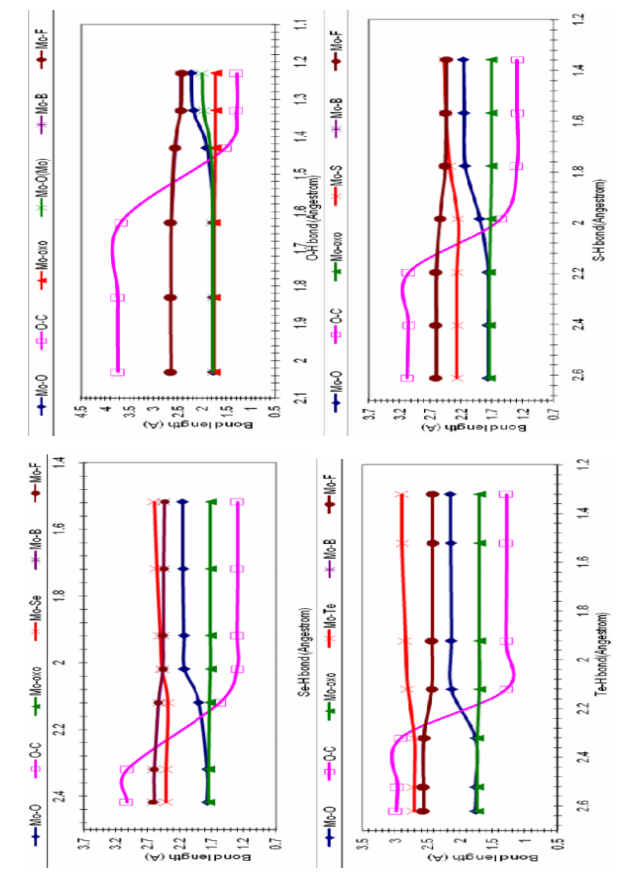

Figure 3.3: Bond length Profile from linear transit calculation.

Terminal of active site	Energy of reactants (kcal/mol)		Energy of TS (kcal/mol)		Energy of products (kcal/mol)		% of extend of Mo-X bond
	E(CH_3CHO + active site)	ZPE	E(transition state structure)	ZPE	E(CH_3COOH + active site)	ZPE	
Oxo	-878656.88	0	-878222.97	433.923	-924610.38	-45953.50	2.575
sulfido	-1081330.69	0	-1080908.95	421.741	-1127383.71	-46053.02	0.693
selenido	-2336818.81	0	-2336399.53	419.284	-2382930.13	-46111.32	0.983
tellerido	-836513.312	0	-836110.25	403.057	-882592.68	-46079.37	0.318

Table 1: The total energy and normalized energies for reactants, transition state and products of the active sites with oxo, sulfido, sellenido and tellurido terminals reacting with acetaldehyde along with the extent of Mo-X bond elongation.

with sulfido terminal, the increase in mulliken charge were 0.142175 to -0.013786 shown in Figure and for complexes with tellerido terminal it was from 0.110400 to -0.202199. But in the case of complex with oxo terminal, the negative mulliken charge on the $H_{acetaldehyde}$ decrease as it travels from $C_{acetaldehyde}$ of the substrate towards the O_{Mo} terminal as 0.155155 to 0.155106. So this could be an indication for the loose in reactivity of complexes with oxo terminal. The differences in properties of the four complexes lie in the details of the Mo-X bond lengths and energy profile in the four transitions states. The largest differences are found in the Mo-X bond lengths: 1.779 Aº in the complexes of active site with O terminal to 2.266 Aº in the S, 2.409A° in the Se and 2.713 Aº in the Te. Interestingly, the extent of Mo-X bond elongation in the transition state follows the opposite trend: the Mo-Te bond extends by only 0.3180 %. The corresponding values for the complexes with Se, S and O terminal were 0.9826, 0.693 and 2.575%, respectively as shown in (Table 1) below. The complex with oxo terminal was thus required significantly larger relative deformation energy in forming the transition state. The bond between the equatorial oxygen of the active site and the carbon being attacked by the equatorial oxygen is 3.74194 A° for complex with oxo terminal which is significantly longer than the rest, i.e.; 3.07976, 3.0220, 1.75784 A° for complexes with S, Se and Te terminal respectively. This indicates weaker Coulombic interaction between the Mo-OH oxygen and the carbonyl carbon of substrate and suggests an earlier, higher-energy transition state for the complex of active sites with oxo terminal relative to the complexes with S, Se or Te terminal. The energy barrier to the transition state reported by PredragIlich and Russ Hille for complexes with oxo, sulfido and tellerido terminals were 91, 78 and 75 kcal/mol (normalized energies) respectively (23). But in this work it has been found that the normalized energies for complexes with oxo, sulfido, sellenido and tellerido terminals were 433.923, 421.742, 419.284 and 403.0578 kcal/mol respectively. The decreasing trend found was the same, though the magnitudes of the energies differ significantly. The complex with oxo terminal again shows considerably maximum energy barrier of ZPE equals 433.923 kcal/mol as shown in (Table 1). Complexes with oxo terminal have highest frequency while complexes with tellerido terminal have lowest frequency. Thus we can observe that the one having higher frequency showed lower reactivity and vice versa.

Conclusion

The properties of complexes with active sites with oxo, sulfido, sellenido and tellerido terminal studied to establish the mechanistic determinants for reaction with acetaldehyde. The differences in properties of the four complexes lie in the details of the Mo-X bond lengths and energy profile in the four transitions states. The complex with oxo terminal required significantly larger relative deformation energy in forming the transition state. This was confirmed by its high extent of Mo-X bond elongation, decreased Mulliken charge on $H_{acetaldehyde}$ along its way towards O_{Mo}, highest frequency and shows considerably maximum energy barrier to the transition state. In addition, long bond distances between O_{eq}-$C_{acetaldehyde}$ during nucleophillic attack explain weaker Coulombic interaction between the Mo-O_{eq} and the carbonyl carbon of substrate and suggest an earlier, higher-energy transition state for the complex. These factors combine to lose reactivity in the "desulfo" form of the enzyme where S has been replaced by O in XOR. The transition state for the active site with tellurido terminal gave lowest energy barrier, lowest Mo-Te bond extend, smallest bond distance between attacking O_{eq} of the active site and $C_{acetaldehyde}$ and there was increased negative Mulliken charge on $H_{acetaldehyde}$. These results gave clue for its existence in nature and that a tellurido form of the enzyme have better catalyzing ability upon oxidation of simple aldehydes. But due to big size of tellurium atom, there might be steric hindrance for big heterocyclic substrates. The better coulombic interaction between O_{eq} and $C_{acetaldehyde}$ in addition to lower energy barrier to the transition state makes the active site with sellenido terminal better reactive than with sulfido terminal. The reactivity of the active site towards acetaldehyde for its oxidation increases from active site with oxo to tellurido terminal.

Competing Interests

The absence of some spectroscopic and chromatographic techniques hindered from better results.

Acknowledgment

I would like to give thanks to Science faculty of Arbaminch University for granting and fully funding the project. Besides, my appreciation should be forwarded to Mrs. Nitsuh Wubeshet and staff members of the digital library of the university.

References

1. Rees DC (2002) Great metalloclusters in enzymology. Annu Rev Biochem 71: 221-246.
2. Enemark JH, Young Ch (1993) Bioinorganic Chemistry of Pterin-Containing Molybdenum and Tungsten Enzymes. G AdV Inorg Chem 40: 1.
3. Holm Coord RH (1990) The biologically relevant oxygen atom transfer chemistry of molybdenum: from synthetic analog systems to enzymes. Chem ReV 100: 183.
4. Stiefel EI (1977) The coordination and bioinorganic chemistry of molybdenum. Prog Inorg Chem 22: 1.
5. Bray RC (1980) The reactions and the structures of molybdenum centers in enzymes. AdV Enzymol Relat Areas Mol Biol 51: 107.
6. Hille R (1994) The reaction mechanism of oxomolybdenum enzymes. Biochem Biophys Acta 1184: 143.
7. Hille R, Stiefel EI, Coucouvanis D, Newton WE (1993) Molybdenum Enzymes, Cofactors and Model Systems. ACS Symposium Series 535, American Chemical Society 22.
8. Alexander Voityuk A, Katrin Albert, Maria Roma˜o J, Robert Huber, Notker Rolsch (1998) Inorg Chem37:176-180.

9. Hille R (1996) The Mononuclear Molybdenum Enzymes. Chem ReV 96: 2757.

10. Joshi HK, Cooney JJ, Inscor FE, Gruhn NE, Lichtenberger DL et al. (2003) Investigation of metal-dithiolate fold angle effects: implications for molybdenum and tungsten enzymes. Proc Natl Acad Sci, U.S.A 100: 3719-3724.

11. Holm Coord RH (1990) The biologically relevant oxygen atom transfer chemistry of molybdenum: from synthetic analog systems to enzymes. Chem ReV 100: 183.

12. Enemark JH, Cooney JJA, Wang JJ, Holm RH (2004) Synthetic analogues and reaction systems relevant to the molybdenum and tungsten oxotransferases. Chem ReV 104: 1175-1200.

13. Roma˜o MJ, Archer M, Moura I, Moura JJG, LeGall J et al. (1995) Crystal structure of the xanthine oxidase-related aldehyde oxido-reductase from D gigas. Science 270: 1170.

14. Schindelin H, Kisker C, Hilton J, Rajagopalan KV, Rees DC (1996) Crystal structure of DMSO reductase: redox-linked changes in molybdopterin coordination. Science 272: 1615.

15. Edward Stiefel I (1997) Chemical keys to molybdenum enzymes. J Chem Soc Dalton Trans 3915-3924.

16. Harary I **(**1956) Bacterial degradation of nicotinic acid. Nature 177: 328-329;

17. Stadtman ER, Stadtman TC, Pastan I, Smith LD (1972) Clostridium barkeri sp. N J Bacterio 110: 758-760.

18. Andreesen JR, Fetzner S (2002) The molybdenum-containing hydroxylases of nicotinate, isonicotinate, and nicotine. Syst Met Ions Biol 39: 405-430.

19. Nadine W, Antonio Pierikb J, Abdellatif Ibdah, Russ H, Holger D, (2009) The Mo-Se active site of nicotinate dehydrogenase1. PNAS 27:11055-11060.

20. Hay PJ, Wadt WR (1985) Ab initio effective core potentials for molecular calculations: Potentials for K to Au including the outermost core orbitals. J Chem Phys 82: 299-310.

21. Gladyshev VN, Khangulov SV Stadtman TC Properties of the selenium- and molybdenum-containing nicotinic acid hydroxylase from Clostridium barkeri. J Biochemistry 32: 212-223.

22. Ilich P, Hille R (2002) Oxo, Sulfido, and Tellurido Mo-enedithiolate Models for Xanthine Oxidase and Understanding the Basis of Enzyme Reactivity. J Am Chem Soc 124: 6796-6797.

23. Meany JE (2001) Application of Hammond's postulate. J Chemical Education 2: 204-207.

24. Nishino T (1994) The conversion of xanthine dehydrogenase to xanthine oxidase and the role of the enzyme in reperfusion injury. J Biochem 116: 4 - 6.